



Published in final edited form as:

Invest Ophthalmol Vis Sci. 2007 March ; 48(3): 1389–1400. doi:10.1167/iovs.06-0677.

Molecular and Cellular Alterations Induced by Sustained Expression of Ciliary Neurotrophic Factor in a Mouse Model of Retinitis Pigmentosa

Kun Do Rhee¹, Alberto Ruiz¹, Jacque L. Duncan², William W. Hauswirth^{3,4}, Matthew M. LaVail², Dean Bok^{*,1,5,6}, Xian-Jie Yang^{*,1,5,7}

¹Jules Stein Eye Institute, University of California, Los Angeles, California

²Beckman Vision Center, University of California, San Francisco, California

³Department of Ophthalmology University of Florida College of Medicine, Gainesville, Florida

⁴Powell Gene Therapy Center, University of Florida College of Medicine, Gainesville, Florida

⁵Brain Research Institute, University of California, Los Angeles, California

⁶Department of Neurobiology, University of California, Los Angeles, California

⁷Molecular Biology Institute, University of California, Los Angeles, California

Abstract

PURPOSE.—To characterize molecular and cellular changes induced by sustained expression of ciliary neurotrophic factor (CNTF) in the *rds* mutant mouse retina.

METHODS.—Recombinant adeno-associated virus (rAAV) expressing CNTF was injected subretinally, for transduction of peripherin/*rds*^{+/-} transgenic mice that carry the P216L mutation found in human retinitis pigmentosa. Characterization of retinal neurons and glia was performed by immunocytochemistry with cell-type-specific markers. Activation of signaling molecules was examined by Western blot and immunostaining. Alterations of gene transcription profiles were studied by microarray analyses.

RESULTS.—CNTF viral transduction maintained rhodopsin expression in surviving rod photoreceptors, but greatly reduced both S- and M-opsin normally expressed in cones. In addition, CNTF treatment resulted in increased numbers and dispersion of Müller glia and Chx10-positive bipolar cells within the inner nuclear layer. Persistent CNTF signaling also caused enhanced phosphorylation of STAT1, STAT3, and p42/44 ERK, as well as their levels of expression. Moreover, altered transcription profiles were detected for a large number of genes. Among these, *Crx* and *Nrl* involved in photoreceptor differentiation and several genes involved in phototransduction were suppressed.

*Each of the following is a corresponding author: Xian-Jie Yang, Jules Stein Eye Institute, 100 Stein Plaza, UCLA, Los Angeles, CA 90095; yang@jsei.ucla.edu, Dean Bok, Jules Stein Eye Institute, 100 Stein Plaza, UCLA, Los Angeles, CA 90095; bok@jsei.ucla.edu. Disclosure: **K.D. Rhee**, None; **A. Ruiz**, None; **J.L. Duncan**, None; **W.W. Hauswirth**, Applied Genetic Technologies, Corp. (I, P, C); **M.M. LaVail**, None; **D. Bok**, None; **X.-J. Yang**, None

CONCLUSIONS.—Despite the rescue from cell death, continuous exposure to CNTF changed photoreceptor cell profiles, especially resulting in the loss of cone immunoreactivity. In addition, the Müller glia and bipolar cells became disorganized, and the number of cells expressing Müller and bipolar cell markers increased. Constitutive CNTF production resulted in sustained activation of cytokine signal transduction and altered the expression of a large number of genes. Therefore, stringent regulation of CNTF may be necessary for its therapeutic application in preventing retinal degeneration.

The neurocytokine ciliary neurotrophic factor (CNTF) displays a variety of effects during the development and maintenance of the nervous system. In the developing vertebrate retina, CNTF crucially influences the differentiation of developing photoreceptor cells as it suppresses rhodopsin expression in the rodent retina and enhances cone opsin expression in the chicken retina.^{1–5} In addition, CNTF induces late retinal progenitor cells to express bipolar cell markers and to specialize as Müller glia in postnatal rodent retinas.^{3,6,7} In the mature retina, CNTF is among the most potent neurotrophic factors protecting retinal neurons against degeneration.⁸ To date, CNTF has been shown to prolong photoreceptor survival in a variety of degeneration models including those caused by genetic mutations in different genes and light-induced injury.^{9–16} Furthermore, CNTF is effective in promoting retinal ganglion cell survival and axonal growth in several glaucoma and axotomy models.^{17–23}

CNTF binds to a tripartite receptor complex that activates receptor associated Jak kinases, which in turn phosphorylate the intracellular portion of the receptors and activate multiple downstream signaling components.^{24–26} Activation of the Jak kinases leads to phosphorylation of two members of the signal transducer and activator of transcription (STAT) family: STAT1 and STAT3.²⁷ In addition, CNTF triggers the extracellular signal-regulated kinase (p42/44 ERK)^{28–31} and the phosphatidylinositol 3 kinase-Akt pathways.³² In the developing mouse retina, CNTF stimulation causes differential activation of the Jak-STAT and ERK pathways among progenitor cells and postmitotic neurons.³¹ The suppression of rhodopsin expression by CNTF in postmitotic photoreceptor precursor cells involves the Jak-STAT, but not the ERK pathway.^{31,33,34} In contrast, promotion of a Müller glial cell fate in the neonatal retina by CNTF requires both STAT and ERK activation.⁷ In the mature rodent retina, intravitreal injection of CNTF or its analogue axokine similarly induces the phosphorylation of STAT and ERK proteins; however, this primarily occurs in retinal ganglion cells and Müller glia.^{29,30}

Owing to the significant potential of CNTF as a broad neuroprotective agent for the retina, both viral vector-based and cell-based CNTF delivery approaches have been developed in animal models and were used recently in a clinical trial.³⁵ Nonetheless, the cellular mechanisms of CNTF-dependent neural protection in various retinal degeneration models have not been elucidated. In a mouse model of retinitis pigmentosa (RP) caused by a dominant mutation (P216L) in the *rd*s/peripherin gene,^{36,37} subretinal delivery of a recombinant adeno-associated virus (rAAV) that expresses a secreted CNTF resulted in effective long-term rescue of the photoreceptor cell layer.¹² However, the surviving cells exhibited enlarged nuclei with increased euchromatin. In addition, rAAV-CNTF treated *rd*s/peripherin mutant retinas showed decreased ERG amplitudes in the a-wave of rod

photoreceptors and the b-wave of rod and cone photoreceptors, compared with untreated mutant retinas, thus indicating an adverse effect on retinal function.^{12,13} Similarly, a cellular rescue without functional restoration has been observed in rats carrying dominant rhodopsin mutations.³⁸ Moreover, in normal rabbit retinas treated with high doses of CNTF, the photoreceptor nuclei were increased in size and accompanied by a significantly reduced cone b-wave ERG amplitude.³⁹ To delineate the underlying causes of altered retinal morphology and function, we have performed molecular and cellular analyses of rAAV-CNTF treated *rd*s/peripherin retinas. Our results demonstrate that viral-mediated CNTF expression in the mature retina results in altered retinal organization and abnormal gene expression, as well as persistent and elevated cytokine signaling events. These findings suggest that properly regulated CNTF expression may be essential for preventing retinal degeneration and achieving functional rescue.

MATERIALS AND METHODS

Animals, Virus Preparation, Injection, and Electroretinographic Analysis

All procedures involving the use of mice were in accordance with the guidelines of the ARVO Statement for the Use of Animals in Ophthalmic and Vision Research; the University of California, Los Angeles; and the University of California, San Francisco. A recombinant adeno-associated virus (rAAV) encoding the chicken β -actin promoter (CBA)/CMV enhancer followed by a modified human CNTF cDNA was prepared as described.¹² This recombinant CNTF contains the human growth hormone signal peptide⁴⁰ and S166D/G167H mutations that increase its affinity toward the CNTF receptor- α (CNTFR α).⁴¹ Transgenic mice (*rd*s^{+/-P216L}) of the line 1300³⁶ on a C57BL/6 background were injected subretinally with rAAV-CBA-sDH-CNTF (abbreviated as rAAV-CNTF hereafter) unilaterally between postnatal day (P)23 and P25. The injection procedure including anesthesia, viral titer, and injection volume were identical, as previously described in Bok et al.¹² In total, 37 *rd*s line 1300 animals were injected with rAAV-CNTF. Injected eyes were analyzed by ERG before harvesting at P44, P70 to P72, or P90 to assess retinal function as described.¹² The contralateral noninjected *rd*s eyes and wild-type adult C57BL/6 eyes were used as the control.

Immunohistochemistry and TUNEL Assay

Wild-type C57BL/6, noninjected and rAAV-CNTF injected *rd*s line 1300 eyes were harvested at P70, P72, or P90 and processed as previously described³¹ with minor modifications. Antibodies used are summarized in Table 1. Mice killed with carbon dioxide were immediately fixed by transcardiac perfusion with 4% paraformaldehyde (PFA) in PBS. Eucleated eyes were further fixed in 4% PFA in PBS overnight at 4°C. The cornea and lens were removed before cryoprotection in 30% sucrose/PBS and embedding in OCT. Cryosections of 14- μ m thickness were washed with PBS and incubated with a blocking solution containing DMEM, 10% fetal calf serum, 2% goat serum, 2% donkey serum, and 0.1% Triton X-100 for 1 hour at room temperature. For labeling with anti-phospho-STAT3 and anti-phospho-ERK, cryosections were first washed three times with PBS and then incubated in deionized 95% formamide, 1.5% 20 \times SSC (pH 7.0), for 10 minutes at 70°C before incubation with the blocking solution. For double staining with Chx10 and Cyclin

D3, cryosections were pretreated in antigen retrieval reagent for 5 minutes at 95°C (R&D System, Minneapolis, MN). After blocking, primary antibodies were incubated at 4°C overnight and secondary antibodies at room temperature for 1 hour, each followed with four washes of PBS containing 0.1% Tween 20.³¹ Immunofluorescent signals were captured with a microscope (E800; Nikon, Tokyo, Japan) equipped with a digital camera (SPOT II; Diagnostic Instruments, Sterling Heights, MI). Confocal imaging was performed (LSM 510 or upgraded LSM 410 microscope; Carl Zeiss Meditec, Inc., Dublin, CA) with argon or helium-neon laser. For each antibody, two or more retinas from different individuals at P70, P72, or P90 were used.

For quantification of cell markers, 1.7- or 2.5- μm confocal optical section images were used. A minimum of four eyes ($n = 4$), each with 4 fields derived from different cryosections (total of 16 fields) of the central 30% of the retina were quantified. Commercial software (ImagePro Plus; Media Cybernetics, Silver Spring, MD) was used to measure and analyze the fluorescent signal-positive cells, using the same cutoff thresholds for a given marker. Quantification of marker-positive cells per field is expressed as mean \pm SEM, with $P < 0.05$ considered statistically significant according to the Student's t -test.

TUNEL assay was performed at P44, P70 to P72, or P90, using cryosections and the In Situ Cell Death Detection Kit (Fluorescein; Roche Diagnostics, Indianapolis, IN). The fluorescein-dUTP DNA labeling signals were captured with a microscope (E800; Nikon, Tokyo, Japan) equipped with a digital camera (SPOT II; Diagnostic Instruments).

Western Blot Analyses

Cell lysates of individual P90 retinas were extracted as previously described.³¹ For serial detection with different primary antibodies, nitrocellulose (NC) membranes were stripped by submerging in 50 mL of 100 mM β -mercaptoethanol, 2% SDS, and 62.5 mM Tris-Cl (pH 6.7) at 50°C for 30 minutes. NC blots were washed twice for 10 minutes with PBS at room temperature and processed for another round of detection (Enhanced Chemiluminescence System; GE Healthcare, Piscataway, NJ).

Microarray Analysis

Total retinal RNA from four eyes injected with rAAV-CNTF virus at P23 and four noninjected contralateral eyes was extracted at P90 (RNeasy Protect Mini Kit; Qiagen Inc., Valencia, CA). Equal amounts of total RNA (2 μg) from each retina were processed for one round of linear amplification according to the instructions provided (RiboAmp RNA Amplification Kit; Arcturus Applied Genomics, Sunnyvale, CA). During amplification, a transcript labeling kit (BioArray High Yield RNA Transcript Labeling Kit; ENZO, Farmingdale, NY) was used in conjunction to produce Biotin-labeled single-stranded RNA probes. All RNA measurements were performed with a spectrophotometer (ND-1000; NanoDrop Technologies Inc., Wilmington, DE). The quality and integrity of RNA samples were evaluated by electrophoresis on 1.2% agarose-formaldehyde gels. Before hybridization, fractionation of each labeled probe was analyzed (2100 Bioanalyzer; Agilent Technologies, Foster City, CA). Each labeled RNA probe (10 μg) was individually hybridized (Mouse Genome 430–2.0 Arrays in a Gene Chip Hybridization Oven 640)

followed by washes in a fluidics station (model 450; all from Affymetrix, Santa Clara, CA). Quadruplet arrays were scanned and data were acquired (Scanner 3000 and Gene Chip Operating Software 1.3; Affymetrix). Data analysis was then performed (ArrayAssist Analysis Software; Iobion/Stratagene, La Jolla, CA).

RESULTS

CNTF Reduces Electrophoretographic Responses

In previous work, the same rAAV-CNTF used in the present study resulted in reduced ERG amplitudes when injected subretinally between P23 and P25 and examined at P90.¹² In the present study, of the 19 *rds*^{+/-} mice carrying the P216L mutant transgene³⁶ and injected subretinally, 18 showed significant depression of scotopic and photopic ERG responses (Table 2). The one mouse that had no recordable difference between the two eyes presumably had a failed subretinal injection and was not used to harvest retinas or for immunocytochemistry. Several mutant mice examined at P70 displayed similar reduced ERG amplitudes, but the scotopic a-waves were not as significantly reduced as the other ERG parameters (Table 2).

CNTF Sustains Rod but Not Cone Photoreceptor Opsin Expression

Subretinal delivery of rAAV expressing CNTF caused dramatic improvement of cell survival in *rds* retinas as indicated by the increased thickness of the outer nuclear layer (ONL).¹² To investigate whether the surviving ONL cells maintained differentiated features of photoreceptors, we performed immunofluorescent staining for rod and cone opsins. At P90, the untreated control *rds* retinas had three to four rows of cell nuclei (Fig. 1C) in the ONL with rhodopsin (Rho4D2⁴²) immunostaining signals within the ONL as well as in the outer segments (Fig. 1A), indicating that the residual rod photoreceptor cells at this stage retained their rhodopsin expression. In P90 *rds* retinas treated with rAAV-CNTF at P23, the ONL contained seven to eight rows of cell nuclei (Fig. 1D), and rhodopsin immunostaining signals were detected in most of the ONL cells (Fig. 1B) with intense labeling of the inner and outer segments and aberrant perinuclear distribution in the ONL.

In the untreated *rds*^{+/-P216L} retinas, M-opsin immunostaining detected M-opsin-positive cells distributed in the dorsal and ventral retina (Figs. 1E, 1I). In contrast, S-opsin immunostaining of *rds*^{+/-P216L} retinas showed a ventrally biased distribution of S-cone cells (Figs. 1G, 1K). These results were similar to the patterns of M-cone and S-cone photoreceptor cell distribution in the wild-type mouse retina,⁴³ indicating that *rds* mutant retinas maintained cone photoreceptor cells as late as P90. In rAAV-CNTF treated *rds*^{+/-P216L} retinas, however, the M-opsin positive cone cells were greatly reduced in the ventral retina, with only residual labeled cells detected in the dorsal retina (Figs. 1F, 1J). Similarly, rAAV-CNTF treated retinas were almost entirely devoid of S-opsin staining signals, suggesting the reduction of S-cone immunoreactivity (Figs. 1H, 1L). To examine further whether the CNTF treatment causes a reduction in the number of cone cells or altered expression of cone-specific genes, we also labeled P70 *rds* retinas with anti-cone arrestin antibody⁴⁴ and fluorescence-conjugated peanut agglutinin (PNA). The untreated control *rds* retinas showed cone arrestin labeling in the outer segments, cell somata, and synapses,

similar to that found in the wild-type retinas, whereas rAAV-CNTF-treated retinas displayed a reduced arrestin signal in the ONL and synaptic termini, but retained a low level of arrestin labeling in the outer segments (Supplementary Figs. S1A–S1D, online at <http://www.iovs.org/cgi/content/full/48/3/1389/DC1>). The PNA labeling was also reduced, but was still detectable in rAAV-CNTF-treated retinas (Supplementary Figs. S1E–S1H).

These results suggest that, despite the photoreceptor cell degeneration, the *rds*^{+/-P216L} retinas retained both rod and cone photoreceptor cells. Viral-mediated CNTF expression was effective in sustaining cells with rod photoreceptor features but resulted in suppression of cone-specific genes, including M-opsin, S-opsin, and cone arrestin.

CNTF Causes Activation and Dispersion of Müller Glial Cells

We next examined the influence of rAAV-mediated CNTF expression on the Müller glial cells, which have been shown to contain phosphorylated STAT and ERK protein on transient CNTF stimulation in vivo.^{29,30} In the mature wild-type retina, immunostaining by a Müller glial marker cyclin D3⁴⁵ showed that Müller glial nuclei occupied the central stratum of the inner nuclear layer (INL; Figs. 2A, 2D). Compared with the wild-type retina, the P90 untreated *rds*^{+/-P216L} retinas contained cyclin D3-positive Müller glial nuclei in a slightly dispersed pattern within the INL, with occasional nuclei ectopically located near the outer plexiform layer (OPL; Figs. 2B, 2E).

In P90 rAAV-CNTF treated *rds*^{+/-P216L} retinas, cyclin D3-positive cell nuclei were broadly dispersed throughout the entire INL, with many positioned within the OPL, which is normally devoid of cell nuclei (Figs. 2C, 2F). Furthermore, immunostaining with Müller glial markers glutamine synthetase (GS)⁴⁵ and glial fibrillary acidic protein (GFAP)⁴⁶ revealed a low degree of Müller activation in untreated and a high degree of Müller activation in rAAV-CNTF treated retinas, as indicated by significantly expanded and swollen Müller glial processes throughout all laminar layers of the retina (Figs. 2H–K). In general, the rAAV-CNTF treated *rds* retinas showed an increased thickness in the ONL and INL compared with the untreated *rds* retina (Figs. 2D–F).

We also counted the numbers of cyclin D3-positive cells in the central region of the P90 retinas. Compared with the wild-type retinas, untreated and rAAV-CNTF treated *rds* retinas contained an average increase of 22% and 46%, respectively (Fig. 2G, $n = 2$, total 10 fields per retina). To obtain a more precise quantification, confocal images of noninjected wild-type retinas and P70 *rds* retinas (data not shown) injected with rAAV-CNTF at P23 were also analyzed (Fig. 2G, $n = 4$, 16 fields per retina). The results showed that cyclin D3-positive cells in rAAV-CNTF treated retinas (62.6 ± 3.7 per frame) had increased 56.5% ($P = 0.001$) over wild-type retinas (39.9 ± 1.7 per frame) and 35.6% ($P = 0.027$) over untreated *rds* retinas (46.2 ± 4.3 per frame).

These results suggest that the *rds* retina, while undergoing slow photoreceptor degeneration, harbors reactive Müller glia, and rAAV-CNTF treatment enhances Müller glial activation and mobilization and increases the number of Müller glial marker-positive cells.

CNTF Enhances Chx10-Positive Cell Population

The reduction in ERG b-wave amplitudes caused by rAAV-CNTF injection suggests that CNTF affects cells in the INL. Immunostaining with the bipolar cell marker 115A10⁴⁷ revealed that rAAV-CNTF treatment resulted in a slightly expanded zone occupied by 115A10-labeled cell bodies within the INL (Figs. 3A–C). We next analyzed the labeling pattern of the homeobox protein Chx10, which is expressed by retinal progenitor cells during development and by bipolar neurons in the mature retina.⁴⁸ Chx10 staining patterns were similar between the wild-type and untreated *rd^s+/-P216L* retinas (Figs. 3D, 3E), whereas rAAV-CNTF treatment resulted in a wide dispersion of Chx10-positive cells in the INL (Fig. 3F). Since, under certain conditions, Müller glia may re-enter the proliferative cell cycle and generate new neurons,^{49,50} we tested whether the dispersed Chx10-positive cells co-label with Müller cell markers. Costaining of the two nuclear antigens Chx10 and cyclin D3 showed minimal overlapping but extensive intermingling between the two cell populations in rAAV-CNTF treated *rd^s+/-P216L* retinas (Fig. 3F). To determine whether there was also an increase in the number of Chx10-positive cells, we performed confocal imaging analyses of P70 to P72 *rd^s* retinas, which showed Chx10 expression patterns similar to those found at P90 (Figs. 3H, 3I). Quantification of the cells in the central retina (Fig. 3G, $n = 4$, 16 fields per retina) showed that Chx10-positive cells in rAAV-CNTF treated retinas (84.6 ± 3.4 per frame) had increased 75.2% ($P = 0.001$) over wild-type retinas (48.3 ± 5.3 per frame) and 42.2% ($P = 0.001$) over untreated *rd^s* retinas (59.5 ± 3.2 per frame), respectively. Interestingly, occasional ectopic Chx10-positive cells were detected in the ONL of rAAV-CNTF-treated retinas at this stage (Fig. 3I).

We also evaluated whether CNTF influences other retinal cell types. Immunostaining by an amacrine cell marker AP2 α ⁵¹ detected only a slight disorganization of the amacrine cells in the rAAV-CNTF-treated retinas (Figs. 4A, 4E). Labeling with calbindin revealed more robust immunostaining of cell somata and processes of horizontal cells in the treated retinas (Figs. 4B, 4F). No apparent change in the ganglion cells was detected at P90 with an antibody against Brn3a (Figs. 4C, 4G), a POU domain nuclear protein expressed by differentiated retinal ganglion cells.⁵² Quantitative analyses of confocal images derived from P70 to P72 *rd^s* retinas detected no significant change in the number of Brn3a labeled ganglion cells ($n = 4$, data not shown), confirming the immunostaining results of the P90 *rd^s* retinas.

Therefore, in addition to mobilization and activation of the Müller glia, persistent CNTF expression caused an increase in both the number and dispersion of Chx10-positive cells accompanied by only minor changes of other INL interneurons.

Persistent STAT and ERK Activation by rAAV-CNTF

Previous studies have shown that intravitreal injection of CNTF protein into the adult rodent eye causes enhanced but transient STAT and ERK activation in retinal ganglion cells and Müller glia.^{29,30} To determine whether constitutive CNTF expression causes persistent signaling pathway activation, we examined the phosphorylated status of STAT and ERK proteins. Western blot analyses showed elevated phospho-STAT3 and phospho-STAT1 in rAAV-CNTF treated *rd^s+/-P216L* retinas compared with untreated control retinas (Fig. 5A).

In addition, the total cellular STAT3 and STAT1 protein levels were increased (Fig. 5B). Furthermore, Western blots detected an increase of phospho-ERK1 and ERK2 (Fig. 5C).

In P90 wild-type and untreated *rd*s retinas, phospho-STAT3 immunolabeling did not detect significant levels of signals (Figs. 6A, 6B). However, in contrast to the wild-type retina, anti-phospho-ERK labeling detected dispersed clusters of cells as radial columns in untreated *rd*s^{+/-P126L} retinas (Figs. 6D, 6E). This pattern of labeling was also observed for phospho-ERK and phospho-STAT3 at P70 in untreated *rd*s mutant (data not shown), probably representing spontaneous activation of ERK and STAT3 in a subset of Müller glia. Consistent with Western blot analyses, high levels of phospho-STAT3 and phospho-ERK labeling were detected in rAAV-CNTF-treated P90 retinas in all three cellular layers (Figs. 6C, 6F).

To delineate which cell-type contained activated STAT3 and ERK in rAAV-CNTF-treated retinas, we performed confocal imaging of co-labeled P70 to P72 *rd*s retinas. In noninjected retinas, a low level of phospho-STAT3 signal was detected (Fig. 6J). Consistent with results obtained from P90 retinas, rAAV-CNTF treatment greatly enhanced the levels of phospho-STAT3 in all three cellular layers as well as in the plexiform layers at P70 (Fig. 6K). Merging of 0.8- μ m optical sections demonstrated extensive colocalization of the Müller marker GS and phospho-STAT3 in Müller cell cytoplasm and nuclei within the INL and in Müller glial processes surrounding the photoreceptor cell bodies and terminating at the outer limiting membrane (OLM; Fig. 6K). In addition, phospho-STAT3 labeling signals were also distributed in photoreceptor cells including the inner and outer segments (Fig. 6K). The phospho-ERK signals were mostly detected in the INL and IPL in untreated *rd*s retinas, especially in the Müller glial cell bodies labeled positive for GS (Fig. 6L). CNTF stimulation resulted in elevated ERK phosphorylation among Müller glia, as indicated by strong labeling of their processes in the ONL and OLM (Fig. 6M). In addition, a subset of cells in the ONL contained high levels of phospho-ERK (Fig. 6M).

Together, these results demonstrate a persistent activation of cytokine signaling caused by rAAV-mediated CNTF expression. The nuclei and processes of Müller glia contained phosphorylated STAT3 and ERK proteins. Most of the photoreceptor cells also contained phospho-STAT3, whereas a subset of ONL cells accumulated high levels of phospho-ERK.

Effects of CNTF on Retinal Cell Death

The increased thickness of the ONL in rAAV-CNTF treated *rd*s retina implied a reduction of photoreceptor cell death. Cell apoptosis TUNEL assays revealed very low levels of cell death in the ONL of treated and untreated *rd*s retinas at P44, P70, and P90 (Figs. 7A–D, and data not shown). Instead, increased apoptosis was detected in the ganglion cell layer of rAAV-CNTF-treated P90 samples (Figs. 7A, 7C). However, no significant cell death was detected in the ganglion cell layer at P44 or P70.

Altered Gene Expression at the Transcriptional Level Due to CNTF

To obtain a more comprehensive assessment of the influence of chronic CNTF expression, we performed microarray analyses to examine changes of gene transcription profiles in the retina. Probes derived from RNAs of untreated control and rAAV-CNTF treated *rd*s^{+/-P216L} retinas ($n = 4$ each) were individually hybridized to gene microarrays (Mouse Genome 430

2.0 Arrays; Affymetrix), which contain 45,000 probe sets corresponding to 39,000 transcripts from 34,000 well-characterized mouse genes. Microarray data showed that compared with untreated *rds* retinas, CNTF consistently caused altered expression of a large number of genes. In at least three of four independent trials, 119 genes showed more than a 25% reduction in their transcript levels, whereas 152 genes showed more than a 25% increase in their transcript levels.

Table 3 summarizes 50 selected known genes that showed an increase or decrease in at least three of four individual trials. Among these, several genes involved in phototransduction were downregulated, including *S*-opsin, cone transducin α -sub-unit, rod transducin β 1-subunit, and rod phosphodiesterase- β . In addition, genes implicated in photoreceptor function and diseases such as the crumbs homologue and retinitis pigmentosa-9 homologue also showed reduced transcript levels. Consistent with the observed nuclear morphologic changes in the rAAV-CNTF treated *rds* retinas, altered expression of genes that function in chromatin remodeling and transcription activation such as nucleolin and histone deacetylase were observed. Furthermore, the homeobox protein *Crx* required for photoreceptor differentiation and maintenance^{53–55} and the leucine zipper protein *Nrl* required for rod specification⁵⁶ were decreased. As expected, GFAP transcription was enhanced in rAAV-CNTF treated *rds* retinas. In agreement with the rescuing effects of CNTF treatment, we also detected changes in transcript levels toward blocking cell death and promoting the cell cycle. Moreover, CNTF treatment affected the expression of a considerable number of signaling molecules. Among these, *STAT1*, *STAT3*, and *ERK1* were augmented, whereas *Jak1* was suppressed.

DISCUSSION

In this study, we investigated the molecular and cellular changes associated with viral mediated CNTF expression in a mouse model of RP caused by a mutation in the *rds*/peripherin gene. Sustained CNTF expression induced a persistent elevation of both the *STAT* and *ERK* signaling pathways in the mutant retina. Despite the protection of the photoreceptor cells in the ONL from the effects of the mutant transgene, CNTF caused significant alteration of cellular phenotypes and reorganization of several retinal cell types. Moreover, CNTF treatment resulted in altered levels of transcripts of a large number of genes in the retina.

Several studies to date have shown that CNTF treatment affects normal and mutant retinal functions. Expression of CNTF by rAAV rescues photoreceptors from cell death in the dominant peripherin/*rds*^{+/-P216L} mutant mouse¹² and dominant rhodopsin mutant rats,³⁸ but causes attenuated ERG amplitudes. Furthermore, delivery of CNTF in combination with wild-type peripherin in *Prph2* (*Rd2/Rd2*) mice negates the effect of gene-replacement therapy.¹³ Moreover, a cell-based delivery study in normal rabbits showed that the cone ERG is diminished at higher doses of CNTF.³⁹ Results of immunocytochemical characterization presented here indicate that most of the surviving ONL cells in the *rds* retina have retained the rod photoreceptor identity with rAAV-CNTF treatment. The rescued rods show robust rhodopsin expression by immunocytochemistry, albeit with an aberrant cellular distribution compared with the wild-type. In contrast to the rod opsin, rAAV-CNTF–

transduced *rd*s retinas display a dramatic reduction of both the short wavelength and medium/long wavelength opsins. This reduction of cone opsin immunoreactivity most likely reflects altered gene expression within surviving cone photoreceptors rather than cone-specific cell death (see note added in proof) since the untreated *rd*s retinas at an equivalent age contain an apparently normal distribution of cones, and CNTF-treated retinas still have measurable photopic ERG responses, although the amplitudes are reduced compared with untreated retinas (Table 2; Bok et al.¹²). Furthermore, the rAAV-CNTF treated retinas showed reduced but detectable levels of cone arrestin as well as PNA antigen associated with the cones. In the developing mouse and rat retinas, CNTF can strongly suppress rhodopsin expression in postmitotic photoreceptor precursor cells. However, once differentiating rod photoreceptor cells reach the stage of rhodopsin expression, they are no longer responsive to CNTF inhibition.³ The lack of CNTF suppression of rhodopsin expression in the *rd*s mutant indicates that even persistent CNTF at high levels does not significantly alter the identity of mature rod photoreceptors, consistent with the observed responses of rods during differentiation.³ The suppression of the rod ERG in rAAV-CNTF treated *rd*s retinas (Table 2; Bok et al.¹²) may be attributable to abnormal expression of other phototransduction genes expressed by rods. In contrast, specific effects of CNTF on S- and M-opsin expression in differentiating mammalian retinas have not been reported. In the chicken retina, CNTF has been shown to promote cone opsin expression in a small fraction of developing photoreceptor cells in vitro.^{1,57} The strong inhibitory effect of virally mediated CNTF expression on both cone opsins in the mature retina suggests that perhaps the established cone photoreceptor programs are more susceptible to cytokine influence, at least in the *rd*s mutant mouse model. In fact, even in normal rats, the intravitreal injection of CNTF and the subretinal injection of rAAV-CNTF produce a greater reduction in photopic than in scotopic ERG responses, and these rats show concomitant reduction in visual performance in behavioral tasks in photopic light levels (McGill TJ et al. *IOVS* 2006; 47:ARVO E-Abstract 4815).

Major effects of persistent CNTF expression in the *rd*s mutant retina also include the cellular alteration and reorganization of the INL, where the cell body of retinal interneurons and Müller glia reside. It has been shown previously that Müller glia become reactive in response to mechanical injury, retinal degeneration, and stimulation by growth factors.^{46,58} In the absence of exogenous CNTF, the mutant *rd*s retinas show a mild Müller gliosis, as indicated by increased GFAP expression compared with the wild-type retinas. In contrast, rAAV-CNTF-treated retinas exhibit high levels of GFAP and glutamine synthetase labeling in the activated Müller cell body and processes. Intriguingly, labeling by cyclin D3 also revealed an increased number of Müller glial cells dispersed throughout the INL. Another INL retinal cell type greatly influenced by constitutive CNTF expression appears to be bipolar cells. Similar to its effect on cyclin D3-positive cells, CNTF causes an increase in Chx10-positive cells as well as their dispersion within the INL, and even into the ONL. The disorganization and repositioning of the Müller glia and bipolar cells within rAAV-CNTF-treated *rd*s retinas are striking and may explain the reduced ERG b-waves originating from the INL (Table 2, Bok et al.¹²). The mechanism(s) underlying CNTF-dependent increases of Müller and bipolar marker-positive cells is currently not understood. Of interest, CNTF has been shown to enhance bipolar cell marker expression,^{3,6} stimulate proliferation of the late

retinal progenitors,^{7,58} and promote Müller gliogenesis in the postnatal developing rodent retina in vitro.⁷ However, in transgenic mice, constitutive expression of leukemia inhibitory factor (LIF), a CNTF family of cytokine, does not seem to increase the proportion of bipolar and Müller cells at the expense of rod photoreceptors.⁵⁹ Accumulating evidence to date suggests that in vertebrate retinas, Müller glia have the potential to become a source of neural stem cells, which can be triggered to reenter the cell cycle and generate new neurons when the retina is injured or is challenged by certain growth factors.^{48,49} It is plausible that CNTF or other growth factors released under the influence of CNTF can potentiate endogenous retinal stem cells. However, the slow onset of CNTF expression from the current AAV vector¹² renders the detection of proliferative events difficult. In addition, current data cannot rule out the possibility of retinal cell transdifferentiation.

Sustained CNTF expression does not alter the normal laminar distribution of amacrine and horizontal cells within the INL. Despite elevated cell death in the ganglion cell layer at P90 in CNTF-treated retinas, we did not detect statistically significant changes in the number of ganglion cells in P70 *rd*s retinas. Since Brn3a is an authentic ganglion cell marker, it is possible that the apoptotic cells seen in the ganglion cell layer were displaced amacrine cells or newly generated cells without proper connections. A recent study has shown that CNTF did not prevent ganglion cell death in a dog model for RP.⁶⁰ Therefore, whether CNTF is neuroprotective for ganglion cells under all retinal degenerative conditions remains to be further determined.

In the wild-type mature retina, phospho-STAT3 and phospho-ERK1/2 are at nearly undetectable levels by immunocytochemistry.^{29,31} In the untreated *rd*s mutant retina, antibodies against phospho-ERK and phospho-STAT3 occasionally labeled radial columns that resembled the morphology of a few clustered Müller glia. Such higher than basal level activation of signaling molecules is probably due to the release of endogenous growth factors in the *rd*s retinas. In the CNTF-treated *rd*s retinas, high levels of phospho-STAT3 and phospho-ERK are present throughout the retina. These distribution patterns of activated signaling molecules are very distinct from the transient STAT and ERK phosphorylation reported in the retinal ganglion cells and Müller glia after a single intravitreal CNTF injection.²⁹ Furthermore, both transient and persistent CNTF expression causes not only the phosphorylation of STAT1 and STAT3, but also the elevation of total STATs at the RNA and protein levels. Cytokine signaling is normally subjected to rapid negative feedback controls, in part mediated by the cytokine induced Jak-STAT inhibitor SOCS (suppressors of cytokine signaling) proteins.⁶¹ The high levels of signaling molecules present in the rAAV-treated retinas perhaps reflect the renewable source of the CNTF ligand, which signals constitutively despite the induction of the negative inhibitors.

One important question regarding the mechanism of CNTF-mediated neural protection is whether CNTF directly targets the photoreceptor cells in the mature retina, or acts through intermediate factors. We have previously demonstrated that during development, CNTF directly triggers rapid STAT3 phosphorylation in The suppression of rhodopsin photoreceptor precursors.³¹ To date, several published studies have investigated the presence of CNTFR α in the ONL of various vertebrate retinas.^{62–66}

However, the results have been inconsistent. We show that rAAV-CNTF treatment leads to elevated phospho-STAT3 and phospho-ERK in the ONL among other locations. Phospho-ERK is predominantly distributed in Müller glia and a subset of ONL cells, whereas phospho-STAT3 is localized not only in Müller glial cell bodies and processes but also in most of the photoreceptor cells in the ONL. Although we can conclude that vector-mediated CNTF expression causes accumulation of phospho-STAT3 and phospho-ERK among ONL cells, the presence of phosphorylated signaling proteins in the ONL of the *rd*s retina does not necessarily confirm that mature photoreceptor cells respond directly to CNTF. The involvement of intermediary growth factors in triggering signal transduction in photoreceptors cannot be excluded at this time.

The cellular phenotypes in the *rd*s retina exposed to chronic CNTF treatment are likely to be downstream events resulting from elevated signal transduction and altered gene expression. Indeed, our genomewide survey using mouse gene microarrays allowed us to detect a large number of genes with transcript levels affected by the long-term CNTF treatment. The numbers of genes affected are likely to be underestimated under the experimental conditions, since only those showing consistent changes in at least three of four independent trials are included. Even though the thresholds used (i.e., transcription of <0.75 and >1.25), are not overtly stringent, the detected up- and downregulations are likely to be statistically significant, because each known mouse gene (i.e., probe set) is represented by 8 to 16 distinct hybridization data points on each array. Moreover, immunocytochemistry and Western blots, as well as semiquantitative PCRs (data not shown) have confirmed the expression status of a number of genes. Of interest, after constitutive CNTF exposure, genes associated with both rod and cone phototransduction or structures were reduced, correlating with the observed decrease in both rod and cone ERGs. The downregulation of *Crx* and *Nrl* is consistent with that observed in LIF-overexpressing mice⁶⁷ and may be the underlying cause for changes seen in numerous photoreceptor-specific genes. Our results also agree with a recent study in normal and rod–cone degeneration canine models in which CNTF protected degenerating photoreceptors but reduced expression of some phototransduction proteins, as well as leading to an increased thickness of the inner retina.⁶⁰ The changes in genes associated with chromatin remodeling and transcription activation in part reflect the altered nuclear morphology found in the ONL of several species after CNTF treatment. Moreover, CNTF also alters expression profiles of genes involved in the cell cycle and apoptosis, and a large number of signaling molecules, thus suggesting a broad impact of persistent cytokine signaling on retinal transcription and, consequently, on cellular function.

In conclusion, we have demonstrated that sustained, high-level CNTF treatment causes a multitude of cellular and molecular changes in a mouse model of retinitis pigmentosa. These results suggest that the mature retina is plastic and susceptible to cytokine influences. Therefore, when considering human application, careful regulation of the dosage and duration of CNTF treatment may be needed to achieve pro-longed optimal therapeutic efficacy.

Supplementary Material

Refer to Web version on PubMed Central for supplementary material.

Acknowledgment

The authors thank Douglas Yasumara, Michael T. Matthes, Marcia Lloyd, Xian-Mei Zhang, Vince Chiodo, Kate Donohue-Rolfe, and Carolyn Graybeal for excellent technical support; Cheryl M. Craft for the gift of cone arrestin antibodies; and Robert Molday for the rhodopsin antibody.

Supported by the National Eye Institute (XJY, DB, MML, JLD, WWH); Research to Prevent Blindness (XJY, JLD); the Karl Kirchgessner Foundation (XJY); the Foundation Fighting Blindness (XJY, DB, MML, JLD, WWH); the Macula Vision Research Foundation (WWH); and the Bernard A. Newcomb Fund (JLD).

References

1. Fuhrmann S, Kirsch M, Hofmann HD. Ciliary neurotrophic factor promotes chick photoreceptor development in vitro. *Development*. 1995;121:2695–2706. [PubMed: 7671829]
2. Kirsch M, Fuhrmann S, Wiese A, Hofmann HD. CNTF exerts opposite effects on in vitro development of rat and chick photoreceptors. *Neuroreport*. 1996;7:697–700. [PubMed: 8733724]
3. Ezzeddine ZD, Yang XJ, DeChiara T, Yancopoulos G, Cepko CL. Postmitotic cells fated to become rod photoreceptors can be respecified by CNTF treatment of the retina. *Development*. 1997;124:1055–1067. [PubMed: 9056780]
4. Neophytou C, Vernallis AB, Smith A, Raff MC. Müller-cell-derived leukaemia inhibitory factor arrests rod photoreceptor differentiation at a postmitotic pre-rod stage of development. *Development*. 1997;124:2345–2354. [PubMed: 9199361]
5. Schulz-Key S, Hofmann HD, Beisenherz-Huss C, Barbisch C, Kirsch M. Ciliary neurotrophic factor as a transient negative regulator of rod development in rat retina. *Invest Ophthalmol Vis Sci*. 2002;43:3099–3108. [PubMed: 12202535]
6. Bhattacharya S, Dooley C, Soto F, Madson J, Das AV, Ahmad I. Involvement of Ath3 in CNTF-mediated differentiation of the late retinal progenitors. *Mol Cell Neurosci*. 2004;27:32–43. [PubMed: 15345241]
7. Goureau O, Rhee KD, Yang XJ. Ciliary neurotrophic factor promotes Müller glia differentiation from the postnatal retinal progenitor pool. *Dev Neurosci*. 2004;26:359–370. [PubMed: 15855765]
8. LaVail MM, Unoki K, Yasumura D, Matthes MT, Yancopoulos GD, Steinberg RH. Multiple growth factors, cytokines, and neurotrophins rescue photoreceptors from the damaging effects of constant light. *Proc Natl Acad Sci USA*. 1992;89:11249–11253. [PubMed: 1454803]
9. Cayouette M, Gravel C. Adenovirus-mediated gene transfer of ciliary neurotrophic factor can prevent photoreceptor degeneration in the retinal degeneration (rd) mouse. *Hum Gene Ther*. 1997;8:423–430. [PubMed: 9054517]
10. Cayouette M, Behn D, Sendtner M, Lachapelle P, Gravel C. Intraocular gene transfer of ciliary neurotrophic factor prevents death and increases responsiveness of rod photoreceptors in the retinal degeneration slow mouse. *J Neurosci*. 1998;18:9282–9293. [PubMed: 9801367]
11. Liang FQ, Dejneka NS, Cohen DR, et al. V-mediated delivery of ciliary neurotrophic factor prolongs photoreceptor survival in the rhodopsin knockout mouse. *Mol Ther*. 2001;3:241–248. [PubMed: 11237681]
12. Bok D, Yasumura D, Matthes MT, et al. Effects of adeno-associated virus-vectored ciliary neurotrophic factor on retinal structure and function in mice with a P216L *rd*s/peripherin mutation. *Exp Eye Res*. 2002;74:719–735. [PubMed: 12126945]
13. Schlichtenbrede FC, MacNeil A, Bainbridge JW, et al. Intraocular gene delivery of ciliary neurotrophic factor results in significant loss of retinal function in normal mice and in the Prph2Rd2/Rd2 model of retinal degeneration. *Gene Ther*. 2003;10:523–427. [PubMed: 12621456]
14. Tao W, Wen R, Goddard MB, et al. Encapsulated cell-based delivery of CNTF reduces photoreceptor degeneration in animal models of retinitis pigmentosa. *Invest Ophthalmol Vis Sci*. 2002;43:3292–3298. [PubMed: 12356837]
15. Adamus G, Sugden B, Shiraga S, Timmers AM, Hauswirth WW. Anti-apoptotic effects of CNTF gene transfer on photoreceptor degeneration in experimental antibody-induced retinopathy. *J Autoimmun*. 2003;21:121–129. [PubMed: 12935781]

16. Huang SP, Lin PK, Liu JH, Khor CN, Lee YJ. Intraocular gene transfer of ciliary neurotrophic factor rescues photoreceptor degeneration in RCS rats. *J Biomed Sci.* 2004;11:37–48. [PubMed: 14730208]
17. Meyer-Franke A, Kaplan MR, Pfrieger FW, Barres BA. Characterization of the signaling interactions that promote the survival and growth of developing retinal ganglion cells in culture. *Neuron.* 1995;15:805–819. [PubMed: 7576630]
18. Cui Q, Lu Q, So KF, Yip HK. CNTF, not other trophic factors, promotes axonal regeneration of axotomized retinal ganglion cells in adult hamsters. *Invest Ophthalmol Vis Sci.* 1999;40:760–766. [PubMed: 10067981]
19. Jo SA, Wang E, Benowitz LI. Ciliary neurotrophic factor is an axogenesis factor for retinal ganglion cells. *Neuroscience.* 1999; 89:579–591. [PubMed: 10077337]
20. Cui Q, Harvey AR. CNTF promotes the regrowth of retinal ganglion cell axons into murine peripheral nerve grafts. *Neuroreport.* 2000;11:3999–4002. [PubMed: 11192617]
21. Cui Q, Yip HK, Zhao RC, So KF, Harvey AR. Intraocular elevation of cyclic AMP potentiates ciliary neurotrophic factor-induced regeneration of adult rat retinal ganglion cell axons. *Mol Cell Neurosci.* 2003;22:49–61. [PubMed: 12595238]
22. van Adel BA, Kostic C, Deglon N, Ball AK, Arsenijevic Y. Delivery of ciliary neurotrophic factor via lentiviral-mediated transfer protects axotomized retinal ganglion cells for an extended period of time. *Hum Gene Ther.* 2003;14:103–115. [PubMed: 12614562]
23. Maier K, Rau CR, Storch MK, et al. Ciliary neurotrophic factor protects retinal ganglion cells from secondary cell death during acute autoimmune optic neuritis in rats. *Brain Pathol.* 2004;14: 378–387. [PubMed: 15605985]
24. Ip NY, McClain J, Barrezaeta NX, et al. The alpha component of the CNTF receptor is required for signaling and defines potential CNTF targets in the adult and during development. *Neuron.* 1993; 10:89–102. [PubMed: 8381290]
25. Davis S, Aldrich TH, Stahl N, et al. LIFR beta and gp130 as heterodimerizing signal transducers of the tripartite CNTF receptor. *Science.* 1993;260:1805–1808. [PubMed: 8390097]
26. Stahl N, Boulton TG, Farruggella T, et al. Association and activation of Jak-Tyk kinases by CNTF-LIF-OSM-IL-6 beta receptor components. *Science.* 1994;263:92–95. [PubMed: 8272873]
27. Bonni A, Frank DA, Schindler C, Greenberg ME. Characterization of a pathway for ciliary neurotrophic factor signaling to the nucleus. *Science.* 1993;262:1575–1579. [PubMed: 7504325]
28. Boulton TG, Stahl N, Yancopoulos GD. Ciliary neurotrophic factor/leukemia inhibitory factor/interleukin 6/oncostatin M family of cytokines induces tyrosine phosphorylation of a common set of proteins overlapping those induced by other cytokines and growth factors. *J Biol Chem.* 1994;269:11648–11655. [PubMed: 7512571]
29. Peterson WM, Wang Q, Tzekova R, Wiegand SJ. Ciliary neurotrophic factor and stress stimuli activate the Jak-STAT pathway in retinal neurons and glia. *J Neurosci.* 2000;20:4081–4090. [PubMed: 10818143]
30. Wahlin KJ, Campochiaro PA, Zack DJ, Adler R. Neurotrophic factors cause activation of intracellular signaling pathways in Müller cells and other cells of the inner retina, but not photoreceptors. *Invest Ophthalmol Vis Sci.* 2000;41:927–936. [PubMed: 10711715]
31. Rhee KD, Goureau O, Chen S, Yang XJ. Cytokine-induced activation of signal transducer and activator of transcription in photoreceptor precursors regulates rod differentiation in the developing mouse retina. *J Neurosci.* 2004;24:9779–9788. [PubMed: 15525763]
32. Oh H, Fujio Y, Kunisada K, et al. Activation of phosphatidylinositol 3-kinase through glycoprotein 130 induces protein kinase B and p70 S6 kinase phosphorylation in cardiac myocytes. *J Biol Chem.* 1998;273:9703–9710. [PubMed: 9545305]
33. Ozawa Y, Nakao K, Shimazaki T, et al. Downregulation of STAT3 activation is required for presumptive rod photoreceptor cells to differentiate in the postnatal retina. *Mol Cell Neurosci.* 2004;26: 258–270. [PubMed: 15207851]
34. Zhang SS, Wei J, Qin H, et al. STAT3-mediated signaling in the determination of rod photoreceptor cell fate in mouse retina. *Invest Ophthalmol Vis Sci.* 2004;45:2407–2412. [PubMed: 15223824]

35. Sieving PA, Caruso RC, Tao W, et al. Ciliary neurotrophic factor (CNTF) for human retinal degeneration: phase I trial of CNTF delivered by encapsulated cell intraocular implants. *Proc Natl Acad Sci USA*. 2006;103:3896–3901. [PubMed: 16505355]
36. Kedzierski W, Lloyd M, Birch DG, Bok D, Travis GH. Generation and analysis of transgenic mice expressing P216L-substituted *rd5*/peripherin in rod photoreceptors. *Invest Ophthalmol Vis Sci*. 1997;38:498–509. [PubMed: 9040483]
37. Kedzierski W, Nusinowitz S, Birch D, et al. Deficiency of *rd5*/peripherin causes photoreceptor death in mouse models of digenic and dominant retinitis pigmentosa. *Proc Natl Acad Sci USA*. 2001;98:7718–7723. [PubMed: 11427722]
38. Liang FQ, Aleman TS, Dejneka NS, et al. Long-term protection of retinal structure but not function using RAAV: CNTF in animal models of retinitis pigmentosa. *Mol Ther*. 2001;4:461–472. [PubMed: 11708883]
39. Bush RA, Lei B, Tao W, et al. Encapsulated cell-based intraocular delivery of ciliary neurotrophic factor in normal rabbit: dose-dependent effects on ERG and retinal histology. *Invest Ophthalmol Vis Sci*. 2004;45:2420–2430. [PubMed: 15223826]
40. Rade JJ, Schulick AH, Virmani R, Dichek DA. Local adenoviral-mediated expression of recombinant hirudin reduces neointima formation after arterial injury. *Nat Med*. 1996;2:293–298. [PubMed: 8612227]
41. Saggio I, Gloaguen I, Poiana G, Laufer R. CNTF variants with increased biological potency and receptor selectivity define a functional site of receptor interaction. *EMBO J*. 1995;14:3045–3054. [PubMed: 7621819]
42. Laird DW, Molday RS. Evidence against the role of rhodopsin in rod outer segment binding to RPE cells. *Invest Ophthalmol Vis Sci*. 1988;29:419–428. [PubMed: 3343097]
43. Applebury ML, Antoch MP, Baxter LC, et al. The murine cone photoreceptor: a single cone type expresses both S and M opsins with retinal spatial patterning. *Neuron*. 2000;27:513–523. [PubMed: 11055434]
44. Zhu X, Brown B, Li A, Mears AJ, Swaroop A, Craft CM. GRK1-dependent phosphorylation of S and M opsins and their binding to cone arrestin during cone phototransduction in the mouse retina. *J Neurosci*. 2003;23:6152–6160. [PubMed: 12853434]
45. Hojo M, Ohtsuka T, Hashimoto N, Gradwohl G, Guillemot F, Kageyama R. Glial cell fate specification modulated by the bHLH gene *Hes5* in mouse retina. *Development*. 2000;127:2515–2522. [PubMed: 10821751]
46. Wang Y, Smith SB, Ogilvie JM, McCool DJ, Sarthy V. Ciliary neurotrophic factor induces glial fibrillary acidic protein in retinal Müller cells through the JAK/STAT signal transduction pathway. *Curr Eye Res*. 2002;24:305–312. [PubMed: 12324870]
47. Onoda N, Fujita SC. A monoclonal antibody specific for a subpopulation of retinal bipolar cells in the frog and other vertebrates. *Brain Res*. 1987;416:359–363. [PubMed: 3497690]
48. Burmeister M, Novak J, Liang MY, et al. Ocular retardation mouse caused by *Chx10* homeobox null allele: impaired retinal progenitor proliferation and bipolar cell differentiation. *Nat Genet*. 1996; 12:376–384. [PubMed: 8630490]
49. Fischer AJ, Reh TA. Müller glia are a potential source of neural regeneration in the postnatal chicken retina. *Nat Neurosci*. 2001; 4:247–252. [PubMed: 11224540]
50. Ooto S, Akagi T, Kageyama R, et al. Potential for neural regeneration after neurotoxic injury in the adult mammalian retina. *Proc Natl Acad Sci USA*. 2004;101:13654–13659. [PubMed: 15353594]
51. West-Mays JA, Zhang J, Nottoli T, et al. AP-2alpha transcription factor is required for early morphogenesis of the lens vesicle. *Dev Biol*. 1999;206:46–62. [PubMed: 9918694]
52. Liu W, Khare SL, Liang X, et al. All *Brn3* genes can promote retinal ganglion cell differentiation in the chick. *Development*. 2000;127: 3237–3247. [PubMed: 10887080]
53. Chen S, Wang QL, Nie Z, et al. *Crx*, a novel *Otx*-like paired-homeodomain protein, binds to and transactivates photoreceptor cell-specific genes. *Neuron*. 1997;19:1017–1030. [PubMed: 9390516]
54. Furukawa T, Morrow EM, Cepko CL. *Crx*, a novel *otx*-like homeobox gene, shows photoreceptor-specific expression and regulates photoreceptor differentiation. *Cell*. 1997;91:531–541. [PubMed: 9390562]

55. Furukawa T, Morrow EM, Li T, Davis FC, Cepko CL. Retinopathy and attenuated circadian entrainment in Crx-deficient mice. *Nat Genet.* 1999;23:466–470. [PubMed: 10581037]
56. Mears AJ, Kondo M, Swain PK, et al. A Nrl is required for rod photoreceptor development. *Nat Genet.* 2001;29:447–452. [PubMed: 11694879]
57. Xie HQ, Adler R. Green cone opsin and rhodopsin regulation by CNTF and staurosporine in cultured chick photoreceptors. *Invest Ophthalmol Vis Sci.* 2000;41:4317–4323. [PubMed: 11095633]
58. Dyer MA, Cepko CL. Control of Müller glial cell proliferation and activation following retinal injury. *Nat Neurosci.* 2000;3:873–880. [PubMed: 10966617]
59. Sherry DM, Mitchell R, Li H, Graham DR, Ash JD. Leukemia inhibitory factor inhibits neuronal development and disrupts synaptic organization in the mouse retina. *J Neurosci Res.* 2005;82:316–332. [PubMed: 16206277]
60. Zeiss CJ, Allore HG, Towle V, Tao W. CNTF induces dose-dependent alterations in retinal morphology in normal and rcd-1 canine retina. *Exp Eye Res.* 2006;82:395–404. [PubMed: 16143329]
61. Alexander WS, Hilton DJ. The role of suppressors of cytokine signaling (SOCS) proteins in regulation of the immune response. *Annu Rev Immunol.* 2004;22:503–529. [PubMed: 15032587]
62. Rhee KD, Yang XJ. Expression of cytokine signal transduction components in the postnatal mouse retina. *Mol Vis.* 2003;9:715–722. [PubMed: 14685141]
63. Beltran WA, Zhang Q, Kijas JW, et al. Cloning, mapping, and retinal expression of the canine ciliary neurotrophic factor receptor α (CNTFR α). *Invest Ophthalmol Vis Sci.* 2003;44:3642–3649. [PubMed: 12882818]
64. Valter K, Bisti S, Stone J. Location of CNTFR α on outer segments: evidence of the site of action of CNTF in rat retina. *Brain Res.* 2003;985:169–175. [PubMed: 12967721]
65. Beltran WA, Rohrer H, Aguirre GD. Immunolocalization of ciliary neurotrophic factor receptor alpha (CNTFR α) in mammalian photoreceptor cells. *Mol Vis.* 2005;11:232–244. [PubMed: 15827545]
66. Wahlin KJ, Lim L, Grice EA, Campochiaro PA, Zack DJ, Adler R. A method for analysis of gene expression in isolated mouse photoreceptor and Müller cells. *Mol Vis.* 2004;10:366–375. [PubMed: 15205663]
67. Graham DR, Overbeek PA, Ash JD. Leukemia inhibitory factor blocks expression of Crx and Nrl transcription factors to inhibit photoreceptor differentiation. *Invest Ophthalmol Vis Sci.* 2005; 46:2601–2610. [PubMed: 15980254]

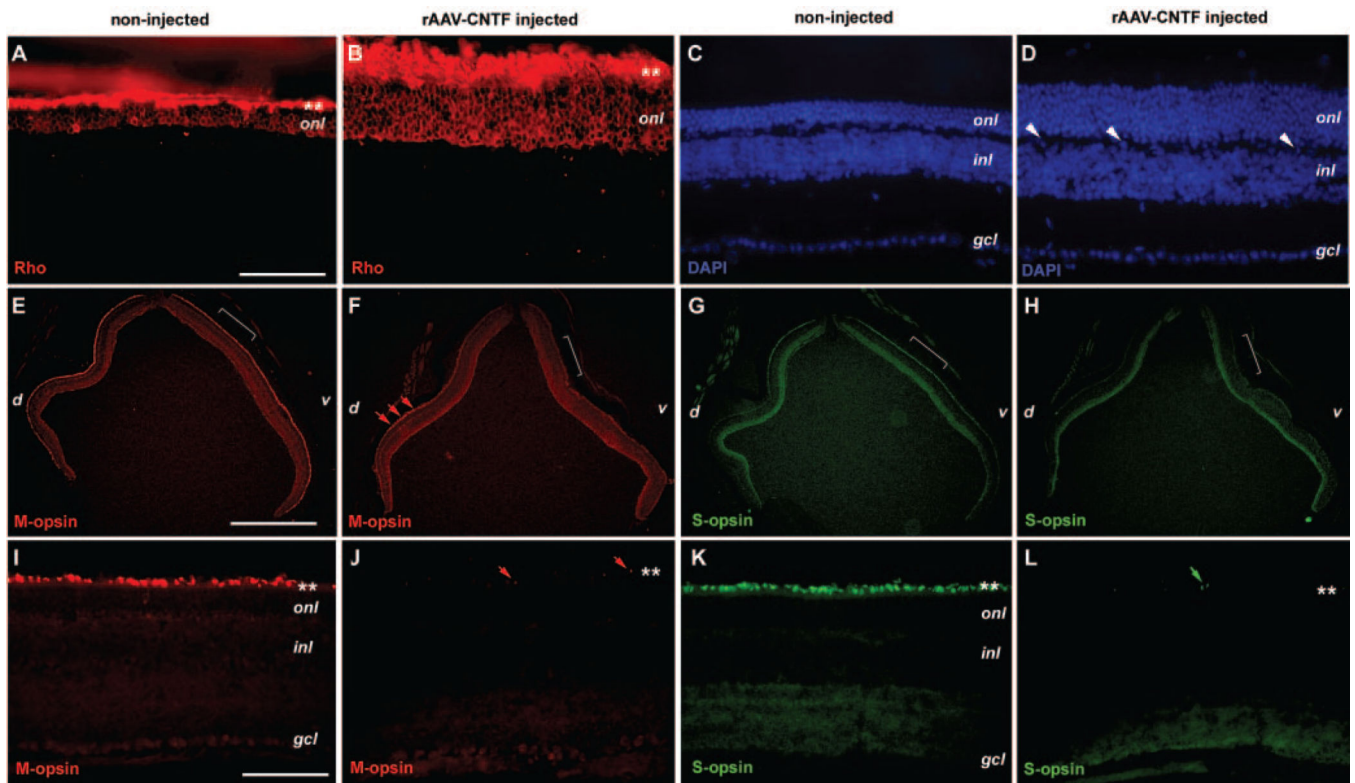
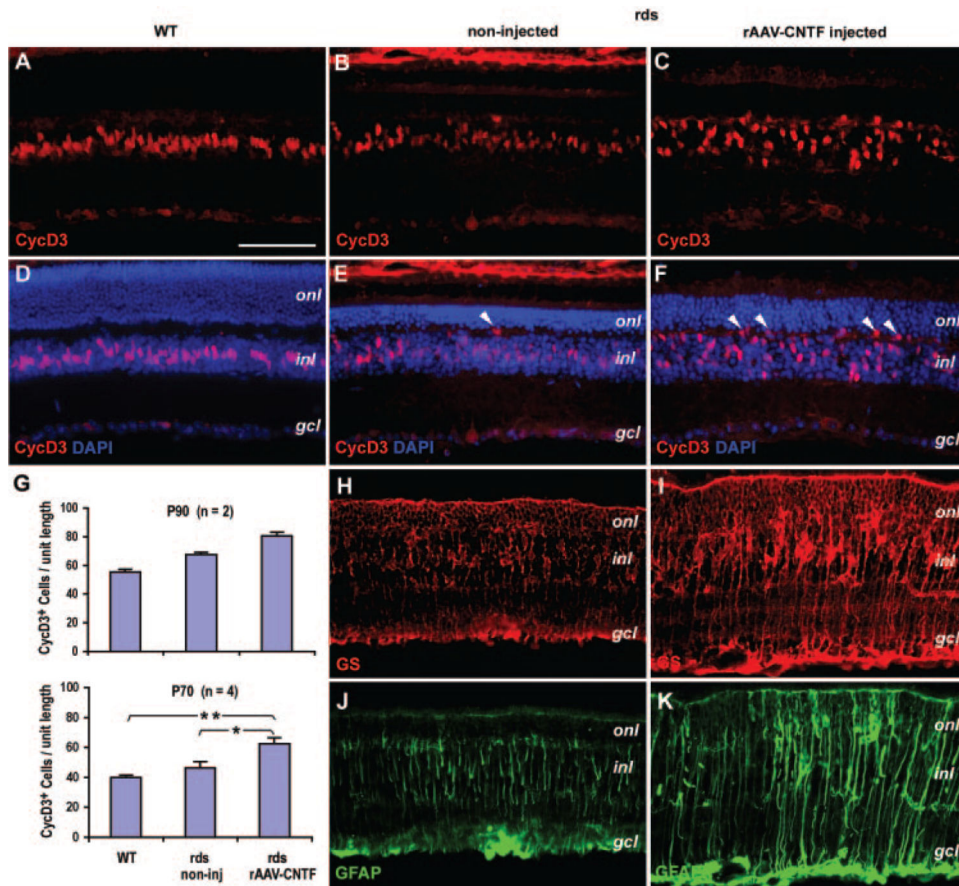


FIGURE 1.

Expression of photoreceptor opsins in the *rds* mutant retina treated with CNTF.

Immunofluorescent images of P90 *rds* retinas treated with rAAV-CNTF at P23 (**B, D, F, H, J, L**) and untreated *rds* control retinas (**A, C, E, G, I, K**) labeled for rhodopsin (**A, B**), M-opsin (**E, F, I, J**), S-opsin (**G, H, K, L**), and 4',6'-diamino-2-phenylindole (DAPI; **C, D**) are shown. (**C**) and (**D**) Corresponding sections to those shown in (**A**) and (**B**). (**D**, *white arrowheads*) Nuclei located in the outer plexiform layer. (**E–H**, *brackets*) Regions enlarged in (**I–L**), respectively. (**F, J**, *red arrows*) Residual M-opsin labeling; (**L**, *green arrows*) residual S-opsin signals. (**A, B, I–L** *) Position of photoreceptor inner and outer segments. d, dorsal; v, ventral; onl, outer nuclear layer; inl, inner nuclear layer; gcl, ganglion cell layer. Scale bars: (**A–D, I–L**) 100 μm ; (**E–H**) 1 mm.

**FIGURE 2.**

Influence of CNTF on Müller glial cells in the *rds* retina. Immunofluorescent images of adult wild-type (WT) retina (**A**, **D**), P90 *rds* retinas treated with rAAV-CNTF at P23 (**C**, **F**, **I**, **K**), and the untreated *rds* control (**B**, **E**, **H**, **J**) labeled for CycD3 (**A–C**), CycD3 and 4',6'-diamino-2-phenylindole (DAPI; **D–F**), GS (**H**, **I**), and GFAP (**J**, **K**) are shown. (**E**, **F**, *white arrowheads*) Ectopic cell nuclei residing in the outer plexiform layer. (**G**) Quantification of CycD3-positive cells at P90 (*top*, $n = 2$, 10 fields each) per unit length of retina (250 μm , at 14- μm thickness) and at P70 (*bottom*, $n = 4$, 16 fields each) per unit length of retina (317 μm , 1.7- μm -thick confocal optical sections). *Statistically significant sample pairs: $P < 0.02$ between untreated and CNTF-treated *rds* retinas, and $P < 0.001$ between wild-type (WT) and CNTF-treated *rds* retinas. onl, outer nuclear layer; inl, inner nuclear layer; gcl, ganglion cell layer. Scale bar, 100 μm .

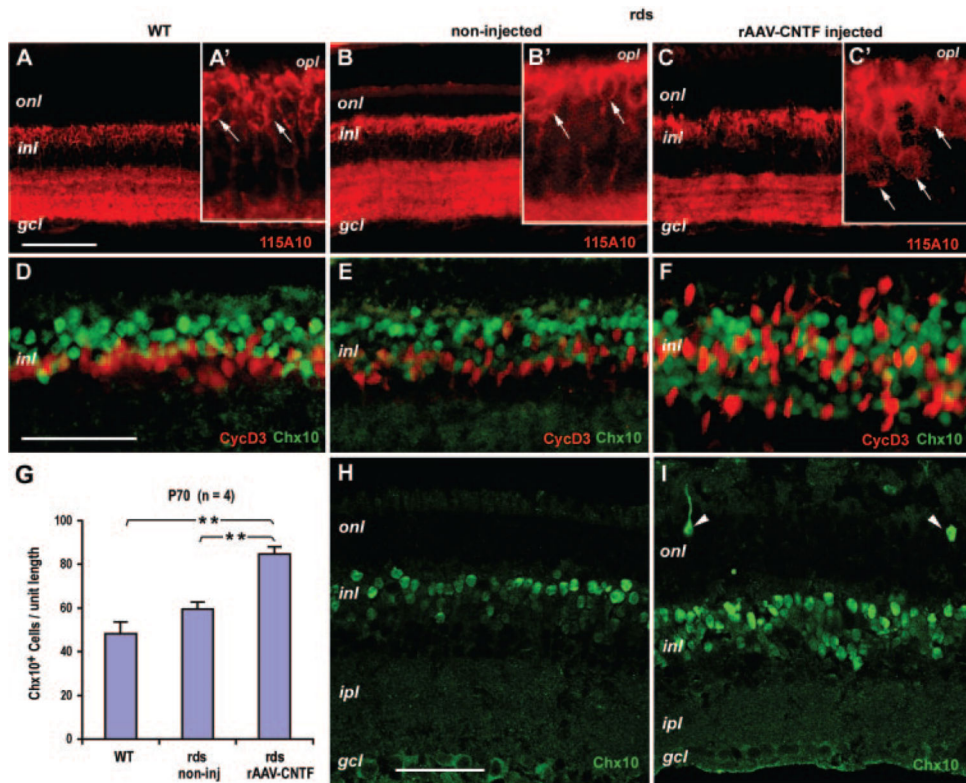


FIGURE 3.

Influence of CNTF on bipolar cells in the *rds* retina. Immunofluorescent images of adult wild-type (WT) retinas (A, D), P90 (B, C, E, F) and P72 (H, I) *rds* retinas treated with rAAV-CNTF at P23 (C, F, I) and the untreated *rds* controls (B, E, H) labeled for 115A10 (A–C; A'–C': higher magnifications of A–C), Chx10 and CycD3 (D–F), and Chx10 (H, I) are shown. (H, I) Examples of the confocal optical sections used for the quantification of Chx10 in (G). (A'–C', white arrows) Cell bodies labeled by 115A10. (I, white arrowheads) Ectopic Chx10-positive cells in the ONL. (G) Quantification of Chx10-positive cells at P70 ($n = 4$, 16 fields each) per unit length (230 μm) of retina (1.7-μm-thick confocal optical sections). *Statistically significant sample pairs: $P < 0.001$ between untreated and CNTF-treated *rds* retinas, and between wild-type (WT) and CNTF-treated *rds* retinas. onl, outer nuclear layer; opl, outer plexiform layer; inl, inner nuclear layer; ipl, inner plexiform layer; gcl, ganglion cell layer. Scale bars: (A–C) 100 μm; (D–F, H, I) 50 μm; (A'–C') magnification of (A–C) ×3.

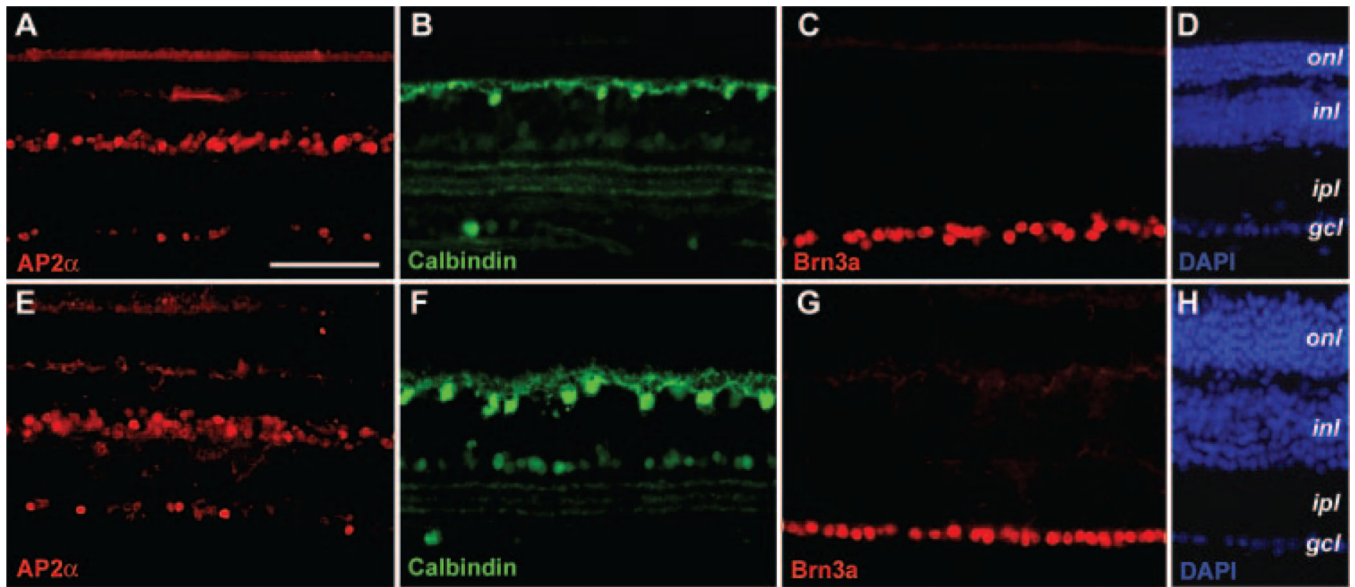


FIGURE 4.

Effects of CNTF on other retinal cell types in the *rds* retina. Immunofluorescent images of P90 *rds* retinal sections treated with rAAV-CNTF at P23 (**E–H**) and the untreated control retinas (**A–D**) labeled for amacrine cell marker AP2 α (**A**, **E**), horizontal cell marker calbindin (**B**, **F**), ganglion cell marker Brn3a (**C**, **G**), and 4',6'-diamino-2-phenylindole (DAPI; **D**, **H**) are shown. Abbreviations as in Figure 3. Scale bar, (**A**) 100 μ m.

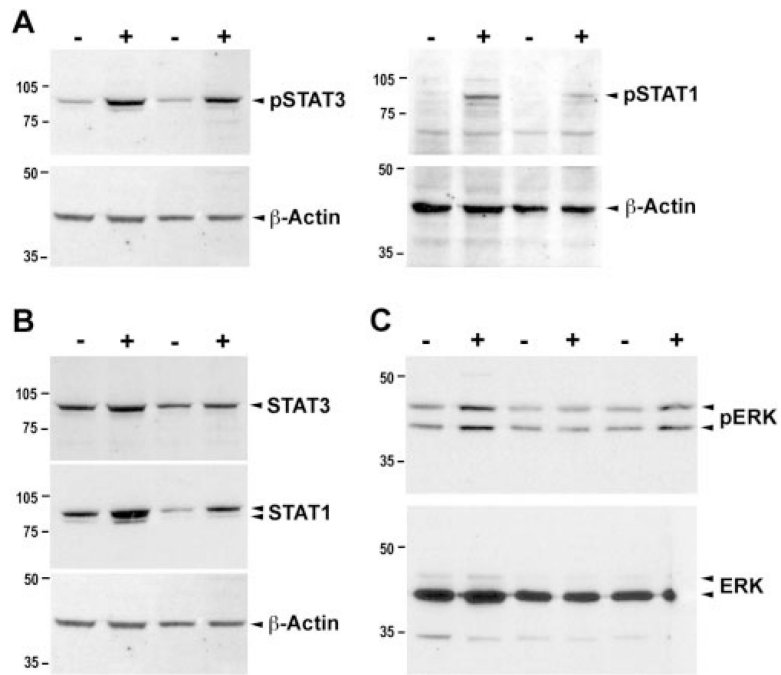


FIGURE 5.

Effects of CNTF on activation and expression of STATs and ERK proteins. Western blot analysis of cell extracts derived from P90 rAAV-CNTF treated (+) and untreated control *rds* retinas (-) are shown. The levels of phospho-STAT1 and phospho-STAT3 (A), the levels of total STAT1 and STAT3 (B), and the levels of phosphorylated p42/44 ERK (C) were all elevated in treated compared with untreated control retinas. *Bottom* panels show β -actin or total ERK as protein loading controls.

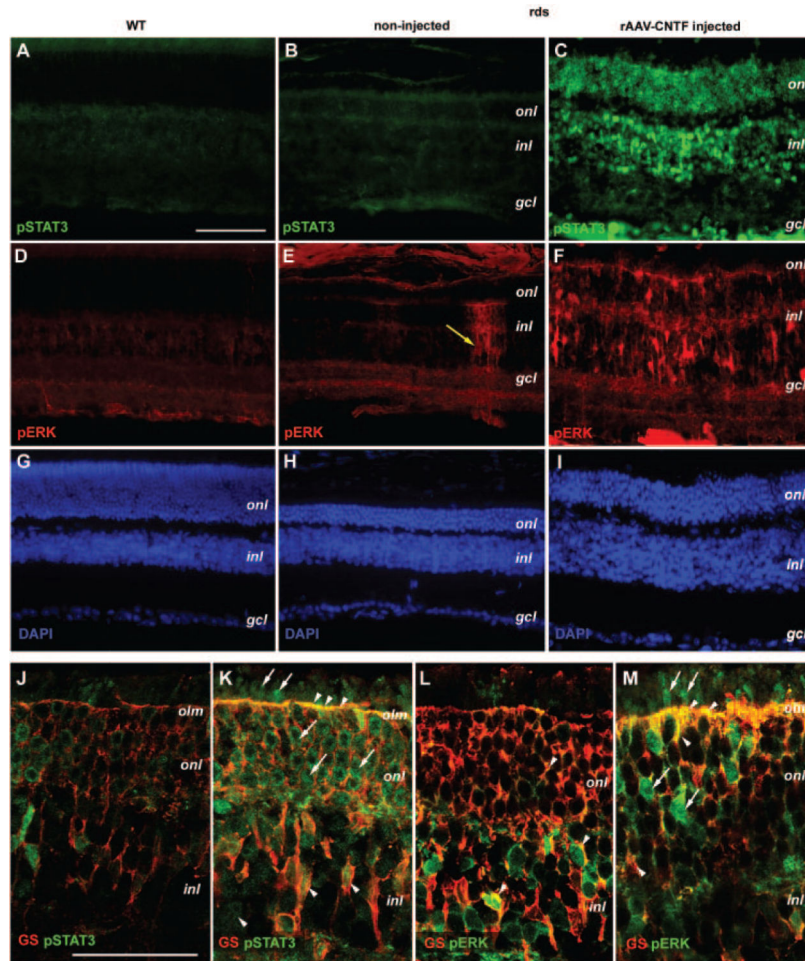


FIGURE 6. Distribution of CNTF-induced phospho-STAT3 and phospho-ERK protein in the *rd*s retina. Immunofluorescent images (A–I) of adult wild-type retina (A, D, G), P90 *rd*s retinas treated with rAAV-CNTF (C, F, I), and the untreated *rd*s control retinas (B, E, H) colabeled for phospho-STAT3 (A–C), phospho-ERK1/2 (D–F), and 4',6'-diamino-2-phenylindole (DAPI; G–I) are shown. Merged confocal images (J–M; 0.8 μ m) of P70 *rd*s retinas treated with rAAV-CNTF (K, M) and the untreated control retinas (J, L) colabeled with GS and pSTAT3 (J, K) or pERK (L, M) are shown. (E, yellow arrow) Isolated phospho-ERK positive column in an untreated *rd*s retina. (K–M) Arrowheads: colabeling of GS and pSTAT3 or pERK; arrows: pSTAT3 or pERK signals alone. Abbreviations as in Figure 3. olm, outer limiting membrane. Scale bar: (A–I) 100 μ m; (J–M) 50 μ m.

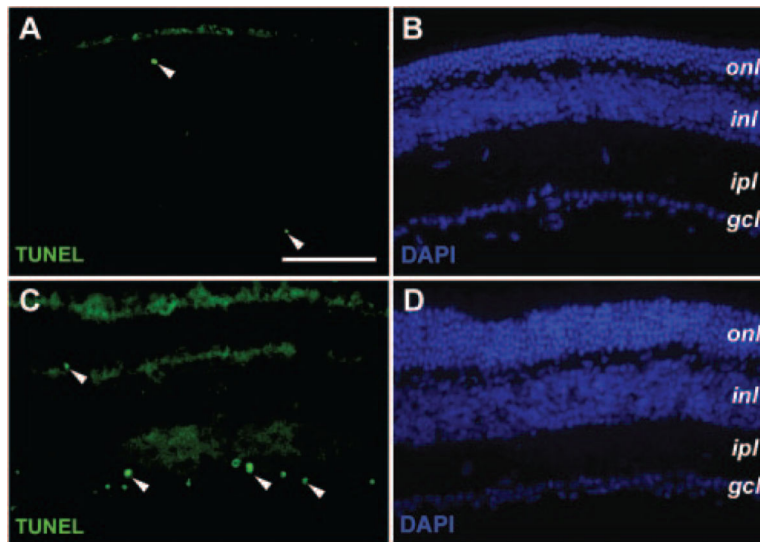


FIGURE 7. Effects of rAAV-CNTF treatment on retinal cell death. Immunofluorescent images of P90 *rds* retinas treated with rAAV-CNTF at P23 (**C, D**) and untreated control retinas (**A, B**) labeled by TUNEL (**A, C**) and 4',6'-diamino-2-phenylindole (DAPI; **B, D**) are shown. (**A, C, arrowheads**) Cells undergoing apoptosis. Increased apoptosis was detected in the ganglion cell layers of the treated P90 *rds* retinas (**C**). Abbreviations as in Figure 3. Scale bar, 100 μm .

TABLE 1.

Summary of Antibodies

Cell Type	Antibody Name	Type	Dilution	Source	Catalog Number
Primary antibodies					
Amacrine cell	AP- α (3B5)	mAb	1:10	DSHB (Univ. of Iowa)	
Bipolar cell	115A10	mAb	1:5	DSHB	
	Chx10	shAb	1:50	Chemicon	AB9014
Ganglion cell	Brn3a	mAb	1:200	Chemicon	MAB1585
Horizontal cell	Calbindin (D-28K)	rAb	1:500	Chemicon	AB1778
Müller glia	Cyclin D3	mAb	1:100	Cell Signaling Inc.	2936
	Glial fibrillary acidic protein (GFAP)	rAb	1:400	Sigma-Aldrich	G 9269
Photoreceptor	Glutamine synthetase (GS)	mAb	1:50	Chemicon	MAB302
	M-opsin	rAb	1:200	Chemicon	ABS405
	Mouse cone arrestin (mCAR)	rAb	1:2000	Cheryl M. Craft	Ref. 44
	Peanut agglutinin (PNA)		1:250	Vector Laboratories	FL-1071
	Rhodopsin (Rho4D2)	mAb	1:250	Robert Molday	Ref. 42
Signaling molecules	S-opsin	rAb	1:200	Chemicon	ABS407
	ERK2 (C-14)	rAb	1:1000 (wt)	Santa Cruz Biotech.	sc-154
	p-ERK1/2 (Thr202/Tyr204)	rAb	1:100, 1:1000 (wt)	Cell Signaling Inc.	9101
	p-STAT3 (Tyr705)	rAb	1:100, 1:1000 (wt)	Cell Signaling Inc.	9171
	p-STAT1 (Tyr701)	rAb	1:1000 (wt)	Cell Signaling Inc.	9131
	STAT1 (p84/p91)	rAb	1:1000 (wt)	Santa Cruz Biotech.	sc-346
	STAT3 (K-15)	rAb	1:1000 (wt)	Cell Signaling Inc.	9132
Secondary antibodies					
	Alexa 488 conjugated	dAb	1:500	Invitrogen/Molecular Probes	A11015
	Alexa 488 conjugated	gAb	1:500	Invitrogen/Molecular Probes	A11008
	Alexa 568 conjugated	gAb	1:500	Invitrogen/Molecular Probes	A11004
	HRP conjugated	shAb	1:1000 (w)	GE Healthcare	NA931V
	HRP conjugated	dAb	1:1000 (w)	GE Healthcare	NA934V
Other	Propidium iodide (PI)		3.3 μ g/mL	Invitrogen/Molecular Probes	P-3566

Author Manuscript

Author Manuscript

Author Manuscript

Author Manuscript

Catalog Number	Source	Dilution	Type	Antibody Name	Cell Type
	Sigma-Aldrich	1.0 μ g/mL		4',6-Diamidino-2-phenylindole (DAPI)	

TABLE 2.

ERG Analysis

Age	n	% Reduction Compared with Control Eye*		
		Scotopic a-Wave	Scotopic b-Wave	Photopic b-Wave
P70-P72	4	16.4 ± 8.5	68.9 ± 8.0	70.8 ± 14.7
<i>P</i>		NS	< 0.03	< 0.02
P90	18	63.7 ± 9.4	81.3 ± 5.5	83.0 ± 4.3
<i>P</i>		< 5 × 10 ⁻⁵	< 5 × 10 ⁻⁸	< 5 × 10 ⁻¹⁰

Both eyes of mice were recorded simultaneously, and the differences between the two eyes were assessed using a two-tailed, paired Student's *t*-test.

* Mean ± SEM.

TABLE 3.

Representative Gene Expression Changes in rAAV-CNTF-Treated *rd*s Retina*

Potential or Known Function	Gene Name	GenBank Acc. Number	Ratios (Mean ± SEM) [†] (rAAV-CNTF Inj./Non-inj.)	
Phototransduction	S-opsin	NM 007538	0.40 ± 0.11	
	Cone transducin alpha-subunit (Gnat2)	NM 008141	0.51 ± 0.01	
	Rod phosphodiesterase b (pdeb)	NM 008806	0.67 ± 0.09	
	Rod transducin beta1-subunit (Gnb1)	NM 008142	0.39 ± 0.13	
	Guanylate cyclase activator 1α (Guca1a)	NM 008189	0.47 ± 0.12	
	Crumbs homolog 1 (crb1)	NM 133239	0.66 ± 0.07	
	Elongation of long chain fatty acids, ELOVL6	BC 100576	0.58 ± 0.08	
	Synapsin II (Syn2)	NM 013680	0.66 ± 0.02	
	Retinitis pigmentosa 9 homolog (RP9)	BC 048480	0.55 ± 0.07	
	Retinol dehydrogenase 11 (Rdh11)	NM 021557	0.60 ± 0.001	
Retinal structure and Function	Interphotoreceptor matrix proteoglycan 1 (Impg1)	NM 022016	1.47 ± 0.10	
	Nestin	NM 016701	1.71 ± 0.13	
	GFAP	NM 010277	2.60 ± 0.98	
	Nucleolin (Ncl)	NM 010880	0.64 ± 0.05	
	Retinoblastoma binding protein 9 (Rbbp9)	NM 015754	0.59 ± 0.10	
	Early growth response 1 (egr1)	NM 007913	0.45 ± 0.03	
	Histone deacetylase 11 (Hdac11)	NM 144919	1.28 ± 0.02	
	Cone rod homeobox gene (Crx)	NM 007770	0.71 ± 0.08	
	Neural retina leucine zipper gene (Nrl)	NM 008736	0.66 ± 0.08	
	Trans-acting transcription factor 1 (SP1)	NM 013672	0.59 ± 0.02	
Transcription	Kruppel-like factor 4 (Klf4)	NM 010637	0.48 ± 0.08	
	Interleukine enhancer binding factor 2 (Ilf2)	NM 026374	0.53 ± 0.07	
	Hairy/enhancer-of-split related with YRPW2 (Hey2)	NM 013904	1.77 ± 0.07	
	Programmed cell death protein 7 (pdcd7)	BC 022772	0.66 ± 0.07	
	Programmed cell death protein 4 (pdcd4)	BC 055739	0.61 ± 0.04	
	Bcl2-like 10 (Bcl2l10)	NM 013479	1.54 ± 0.06	
	Annexin A7 (Anxa7)	NM 009674	0.62 ± 0.08	
	Transducer of ERBB2, 2 (Tob2)	NM 020507	0.66 ± 0.04	
	Cell death/survival	Programmed cell death protein 7 (pdcd7)	BC 022772	0.66 ± 0.07
		Programmed cell death protein 4 (pdcd4)	BC 055739	0.61 ± 0.04
Bcl2-like 10 (Bcl2l10)		NM 013479	1.54 ± 0.06	
Annexin A7 (Anxa7)		NM 009674	0.62 ± 0.08	
Transducer of ERBB2, 2 (Tob2)		NM 020507	0.66 ± 0.04	
Cell cycle		Programmed cell death protein 7 (pdcd7)	BC 022772	0.66 ± 0.07
		Programmed cell death protein 4 (pdcd4)	BC 055739	0.61 ± 0.04
		Bcl2-like 10 (Bcl2l10)	NM 013479	1.54 ± 0.06
		Annexin A7 (Anxa7)	NM 009674	0.62 ± 0.08
		Transducer of ERBB2, 2 (Tob2)	NM 020507	0.66 ± 0.04
	Cell cycle	Programmed cell death protein 7 (pdcd7)	BC 022772	0.66 ± 0.07
		Programmed cell death protein 4 (pdcd4)	BC 055739	0.61 ± 0.04
		Bcl2-like 10 (Bcl2l10)	NM 013479	1.54 ± 0.06
		Annexin A7 (Anxa7)	NM 009674	0.62 ± 0.08
		Transducer of ERBB2, 2 (Tob2)	NM 020507	0.66 ± 0.04
Cell cycle		Programmed cell death protein 7 (pdcd7)	BC 022772	0.66 ± 0.07
		Programmed cell death protein 4 (pdcd4)	BC 055739	0.61 ± 0.04
		Bcl2-like 10 (Bcl2l10)	NM 013479	1.54 ± 0.06
		Annexin A7 (Anxa7)	NM 009674	0.62 ± 0.08
		Transducer of ERBB2, 2 (Tob2)	NM 020507	0.66 ± 0.04
	Cell cycle	Programmed cell death protein 7 (pdcd7)	BC 022772	0.66 ± 0.07
		Programmed cell death protein 4 (pdcd4)	BC 055739	0.61 ± 0.04
		Bcl2-like 10 (Bcl2l10)	NM 013479	1.54 ± 0.06
		Annexin A7 (Anxa7)	NM 009674	0.62 ± 0.08
		Transducer of ERBB2, 2 (Tob2)	NM 020507	0.66 ± 0.04
Cell cycle		Programmed cell death protein 7 (pdcd7)	BC 022772	0.66 ± 0.07
		Programmed cell death protein 4 (pdcd4)	BC 055739	0.61 ± 0.04
		Bcl2-like 10 (Bcl2l10)	NM 013479	1.54 ± 0.06
		Annexin A7 (Anxa7)	NM 009674	0.62 ± 0.08
		Transducer of ERBB2, 2 (Tob2)	NM 020507	0.66 ± 0.04

Potential or Known Function	Gene Name	GenBank Acc. Number	Ratios (Mean \pm SEM) [†] (rAAV-CNTF inj./Non-inj.)
	Wee 1 homolog	NM 009516	1.68 \pm 0.20
	G1 to phase transition 1 (Gsp1)	NM 146066	1.57 \pm 0.12
	Neuroblastoma myc-related oncogene 1 (Nmyc)	NM 008709	1.56 \pm 0.10
	Cyclin-dependent kinase-like 3 (Cdkl3)	NM 153785	1.35 \pm 0.07
Signal transduction	Janus kinase 1 (Jak1)	NM 146145	0.65 \pm 0.03
	Ephrin B2 (Efnb2)	NM 010111	0.48 \pm 0.07
	SH2 domain binding protein 1 (Sh2bp1)	BC 071247	0.56 \pm 0.06
	Cellular repressor of E1A-stimulated genes (Creg1)	NM 011804	0.67 \pm 0.06
	Protein tyrosine phosphatase, receptor type, E (Ptpre)	NM 011212	0.59 \pm 0.03
	Protein tyrosine phosphatase, non-receptor 21 (Ptpn21)	NM 011877	0.69 \pm 0.03
	STAT1	NM 009283	1.65 \pm 0.14
	Smoothened (Smo)	BC 048091	0.65 \pm 0.02
	STAT3	NM 011486	1.60 \pm 0.40
	MAPK1	NM 011949	1.78 \pm 0.25
	MAPK-interacting ser/threo kinase 1 (Mknk1)	BC 021369	1.48 \pm 0.12
	Serum/glucocorticoid regulated kinase 2 (Sgk2)	NM 013731	1.47 \pm 0.14
	Neuropilin 1 (Nrp1)	NM 008737	1.52 \pm 0.17
	Growth hormone receptor (Ghr)	NM 010284	1.65 \pm 0.36
	Platelet derived growth factor, alpha (Pdgfa)	NM 008808	1.66 \pm 0.22
	Chemokine (C-X-C motif) ligand 13 (Cxcl13)	NM 018866	2.84 \pm 0.37
Immunoresponse	Complement component factor I (Cfi)	NM 007686	1.42 \pm 0.06
	Complement component 4 (C4)	M11789	1.66 \pm 0.66

* A representative 50 genes with transcript levels altered by more than 25% after rAAV-CNTF treatment are shown. Genes with decreased transcripts are listed before genes with increased transcripts in each functional category.

[†]The ratios of rAAV-CNTF injected *rd6* retina and control noninjected *rd6* retina represent values from three or four independent array experiments (mean \pm SEM).